

# Upgrade of the Infrared Camera Diagnostics for the JET ILW divertor

I. Balboa<sup>1</sup>, G. Arnoux<sup>1</sup>, T. Eich<sup>2</sup>, B. Sieglin<sup>2</sup>, S. Devaux<sup>2</sup>, W. Zeidner<sup>2</sup>, C. Morlock<sup>3</sup>, U. Kruezi<sup>3</sup>, G. Sergienko<sup>3</sup>, D. Kinna<sup>1</sup>, P. D. Thomas<sup>1</sup>, M. Rack<sup>3</sup> and JET EFDA contributors\*

JET-EFDA, Culham Science Centre, Abingdon, OX14 3DB, UK

<sup>1</sup>EURATOM/CCFE Fusion Association, Culham Science Centre, Oxon. OX14 3DB, UK  
<sup>2</sup>IPP EURATOM Association FZJ D-52425 Jülich Germany

<sup>3</sup>Max-Planck, EURATOM Association, D-85748 Garching, Germany  
 \* See the Appendix of F. Romanelli et al., Fusion Energy 2010 (Proc. 23rd Int. FEC Daejeon, 2010) IAEA, (2010)

## ABSTRACT

For the new ITER-like wall (ILW) at JET, two new infrared diagnostics (KL9B, KL3B) have been installed. The cameras operate between 3.5-5  $\mu\text{m}$  and up to sampling frequencies of  $\sim 20$  kHz. KL9B and KL3B image the horizontal and vertical tiles of the divertor. The divertor tiles are tungsten coated carbon fibre composite (CFC) except the central tile which is bulk tungsten and consists of lamella segments. The thermal emission from the gaps between the lamellae affects the temperature measurements and therefore KL9A has been upgraded to achieve higher spatial resolution. A technical description of KL9A, KL9B and KL3B and a cross comparison with a near infrared (NIR) camera and 2-colour pyrometer is presented.

## INFRARED THERMOGRAPHY

### Brief Summary

- Imaging of infrared photons emitted from the surface under test producing a visible image
- Camera is sensitive in a limited wavelength range  $\rightarrow$  determines the number of photons collected
- Pixels are quantified in terms of "digital levels" (DLs)
- Calibration using a reference hot source allows to convert from DLs to temperature values

## JET DIVERTOR REGION (see figure 1)

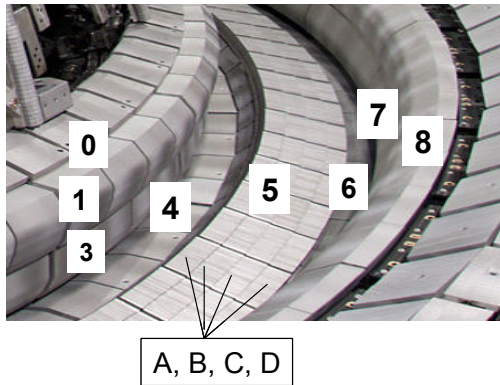


FIG. 1. Diagram of divertor region showing the tile numbers (there is no tile #2). Central tile (#5) is made of bulk tungsten. Other tiles are tungsten coated carbon fibre composite

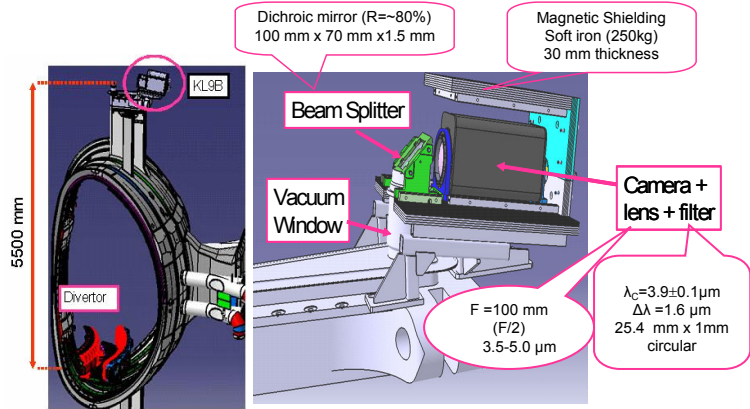


FIG. 2. Left: KL9B layout. Right: Key components of the KL9B diagnostic

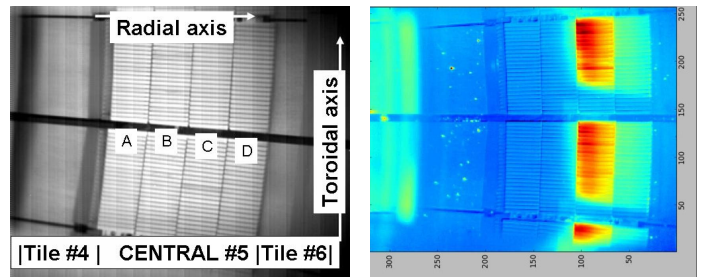


FIG. 3. KL9B's field of view and IR image for JPN82628 (time =63 s) showing the strike line region

## KL3B: NEW INFRARED DIAGNOSTIC FOR THE JET DIVERTOR

- IR camera is a technical twin of the camera for the KL9B diagnostic (i.e. same specifications as for KL9B)
- No magnetic shielding required at this location

Layout (see figure 4)

## KL9B: NEW INFRARED DIAGNOSTIC FOR JET DIVERTOR

### Components Description

- IR camera
- Imaging system
- Power supply
- Cooling
- Magnetic shielding

### Specifications

- IR camera was manufactured at FLIR ATS (<http://www.flir.com>)
- Camera sensor: 320x256 pixels, pixel pitch: 30  $\mu\text{m}$
- Sensor wavelength response: 1.5-5.0  $\mu\text{m}$
- ADC resolution: 14 bits
- Image in grey scale
- Sampling Frequency: up to  $\sim 20$  kHz depending on frame size
- Integration time: down to 3-4  $\mu\text{s}$
- Spatial Resolution: 1.6 mm/pixel
- Dimensions: 400 mm x 110 mm x 170 mm
- Cooling: water pipe fitted on the outside of the back of the camera (closest side to sensor)

### Application

- Study of toroidal asymmetries together with KL9A diagnostic (see page 2). KL9A/B are separated toroidally by 135°

### Layout and Field of View (see figure 2 and 3 respectively)

- KL9B views mainly the central divertor tile from the top of the machine
- Plasma light is imaged through a set of vacuum windows and directed via a beam splitter at 45° into the camera. Distance from the camera to the divertor:  $\sim 5,500$  mm

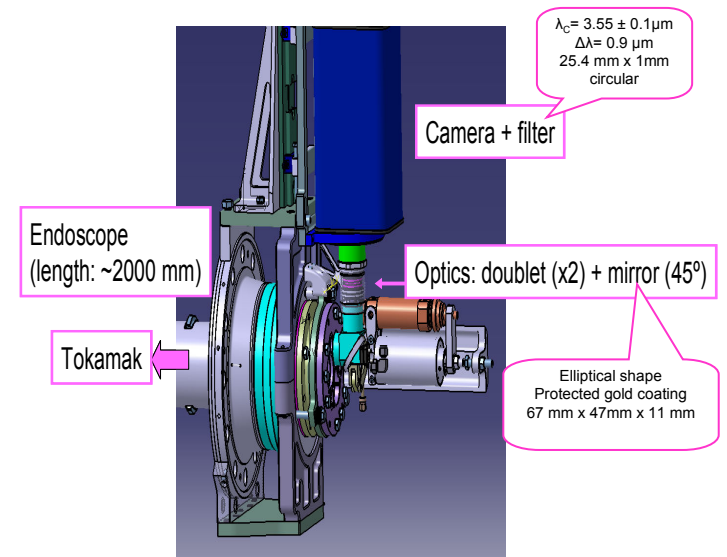


FIG. 4. KL3B layout and key components

# Upgrade of the Infrared Camera Diagnostics for the JET ILW divertor (PAGE 2)

## Field of View (FOV) and Spatial Resolution (see figure 5)

- Prism situated at the "plasma end" of the endoscope: divides FOV into two sections: upper and lower
- Upper section of the FOV: tiles #1, #3, #4 and #5 (Spatial Resolution: 4 mm/pixel)
- Lower section of the FOV: tiles #7 and #8 (Spatial Resolution: 10 mm/pixel)

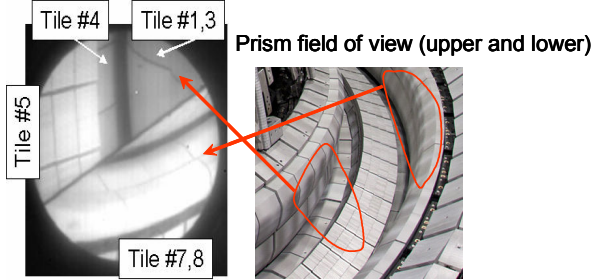


FIG. 5. Left: KL3B's field of view. Right: Prism viewing sections of the divertor region

## KL9A: RECENT UPGRADE OF AN EXISTING DIAGNOSTIC<sup>[1]</sup>

### Motivation & Scope

- Thermal emission from the gaps between lamellae affects the calculation of the heat loads around the edges of the lamellae
- Installation of a new camera lens in order to increase original spatial resolution to 0.8mm/pixel

### Layout and Field of view (see figure 6)

- Same layout than KL9B but it is separated toroidally from KL9B
- Components:
  - Beam splitter: neutral density filter made from quartz (100 mm x 70 mm x 1 mm)
  - Optical filter: Low Pass centred at  $4.2 \pm 0.1 \mu\text{m}$ . Dimensions: 25.4 mm x 1 mm (thickness)
  - New camera lens: focal length= 200 mm (F/2). Wavelength response: 3.5-5  $\mu\text{m}$  (see figure 6)

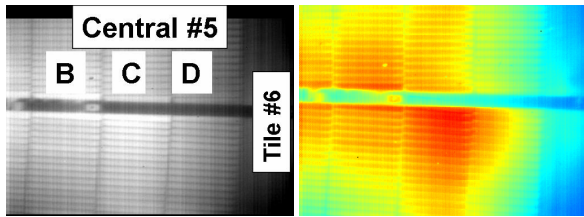


FIG. 6. KL9A field of view after the upgrade and IR image for JPN 82325

## RESULTS

- Cross comparison of KL9B diagnostic with other thermal diagnostics independently calibrated such as NIR cameras and 2-colour pyrometers<sup>[2]</sup>
- The 2-colour pyrometer and the NIR camera chosen for the comparison are the ones which share the same vacuum window as KL9B -> same FOV
- The tungsten emissivity applied for KL9B/KL3B is  $\sim 0.2$  for their wavelength range [2]
- Reflections from other sources are not considered significant for the pulses shown since the ROIs for KL9B and KL3B have been centred around the strike line region (*i.e.* high heat flux) on the divertor tiles

## Comparison of KL9B with a 2-colour pyrometer (KL2D-P8PB) (see figure 7)

- Pyrometers: - 2-colour devices that operate between (350°-1300° C)
  - Spatial averaging over an area of 15 mm diameter
  - Pyrometer KL2D- P8P is centred on lamella #13 of stack C of central tile #5
- KL9B average temperature has been calculated as a function of time for a section which simulates the pyrometer spot but without including the gap between the lamellae
- Reasonable agreement within  $\pm 60^\circ\text{C}$  between the pyrometer KL2D-P8PB and KL9B except for the cooling phase

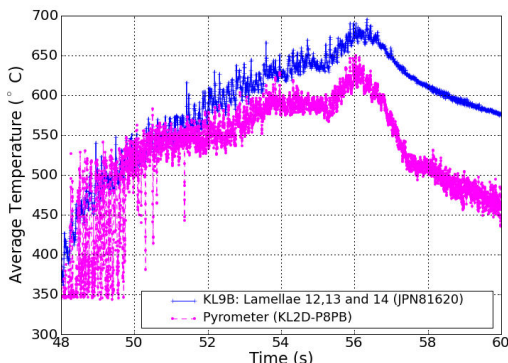


FIG. 7 Comparison of the average temperature between KL9B and pyrometer KL2D-P8PB

## Comparison of KL9B and a near infrared (NIR) camera (KL2D-P8TB) (see figure 8)

- NIR cameras: CCD cameras that operate around  $\sim 1 \mu\text{m}$ . Sampling frequency: 50 Hz
- NIR camera (KL2D-P8TB) has a temperature range between  $850^\circ\text{C}$  -  $1500^\circ\text{C}$
- Good agreement between KL9B and NIR camera (KL2D-P8TB) within  $\pm 50^\circ\text{C}$  above  $850^\circ\text{C}$
- KL9B higher temporal resolution is shown in close up view inside the graph

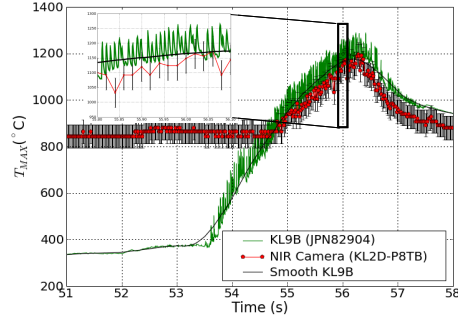


FIG. 8. Comparison of KL9B and NIR protection camera KL2D-P8TB for pulse JPN82904

## Comparison of KL9B versus KL3B (see figure 9)

- Includes the ohmic, NBI heating and cooling phases for pulses JPN82630, 82631, 82643
- Temperature values agreed within  $\pm 50^\circ\text{C}$  (this corresponds to  $2\sigma$  for 22,140 measurement points)
- Variation between the two systems is larger at higher temperatures (above  $800^\circ\text{C}$ ) due to the difference in the spatial resolution between KL3B and KL9B
- For the three pulses edge localized modes (ELMs) can be detected above  $600^\circ\text{C}$

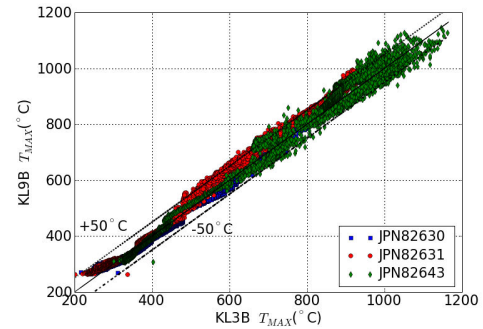


FIG. 9. Comparison between KL9B and KL3B temperature values for JPN82630, 82631 and 82643

## CONCLUSIONS

A technical description of two new infrared diagnostics for the JET divertor has been presented as well as a cross correlation with other thermal diagnostics such as a NIR camera and a 2-colour pyrometer.

## ACKNOWLEDGEMENTS

This work, supported by the European Communities under the contract of Association between EURATOM and CCFE was carried out within the framework of the European Fusion Development Agreement. The views and opinions expressed herein do not necessarily reflect those of the European Commission. The work was also part-funded by the RCUK Energy Programme under grant EP/I501045. Special thanks to J. Wilson, I. Pearson, R. Fenn and C. Rose for their support during the mechanical design assembly modifications and installations.

## REFERENCES

- [1] T. Eich et al., "Type-I ELM power deposition profile width and temporal shape in JET", Journal of Nuclear Materials, **415**, S856-S859 (2011)
- [2] G. Arnoux et al., "A protection system for the JET ITER-like wall based on imaging diagnostics" (submitted at this conference)